Design and fabrication of bi-layer metallic nanowire polarizers and colorfilters based on Surface Plasmon waveguide mode resonances

Zhicheng Ye *[a], Jun Zheng[b], Chenchen Zhang[c], Shu Sun[c]
[a]National Engineering Laboratory for TFT-LCD Technology, Department of Electrical Engineer, Shanghai Jiao Tong University, Shanghai, 200240, China; [b] Key Laboratory for Laser Plasmas (Ministry of Education) and Department of Physics, Shanghai Jiao Tong University, Shanghai 200240, China; [c] Department of Physics, Shanghai Jiao Tong University, Shanghai 200240, China
*Corresponding author: 86-21-34207894 (TEL) , 86-21-34204371 (FAX), yzhch@sjtu.edu.cn

ABSTRACT

Optical responses in Bi-layer metallic nanowire grating are investigated. There are two kinds of Surface Plasmon resonances: lateral propagating Surface Plasmon waveguide modes excited by the diffraction of the grating which lead to dips in transmission; Surface Plasmon resonance between the slits of the grating, which leads to high extinction ration of TM to TE transmission. With simultaneous resonances, a compacted device of integrated color filter and polarizer can be achieved. In order to improve the transmission of TM light, an undercut structure is proposed. The mechanism of the enhancement is analyzed. Bi-layer metallic nanowire gratings are fabricated by laser interference lithography and subsequent E-beam deposition. The measured transmission and reflection spectra confirmed the theoretical and numerical simulations. The results will have wide potential applications in Displays, Optical communication, and integrated Optics.

Keywords: Surface Plasmon, Nanowire Polarizer, Laser Interference Lithography, Waveguide, Liquid Crystal Displays

1. INTRODUCTION

Surface Plasmon Polariton (SPP), electromagnetic wave resonance between the metal and dielectric interface, has become an active topic in the fields of sensors, light emitting devices and optical communication. The localized SPP can increase the sensitivity of sensors [1], the output of light emitting diodes [2] and the absorption of solar cells [3]; the propagating surface plasmon (SP) can be an information carrier in the next generation high integrated optical connection with smaller feature size[4]. Also, extraordinary transmission via the sub-wavelength slits or holes in the metal films [5-7], especially the single layer metallic nanowire gratings [8] is of great interest in liquid crystal displays (LCDs) [9] . It has been proved both in theory and experiment that the SP waveguide resonance inside the metal openings, leads to the efficient transmission of TM light. In order to obtain high extinction ratio of TM to TE light in wide spectra, the pitch of the grating should be small enough to maintain the single mode condition of the slit waveguides only for the TM light and the smaller the pitch the better transmission is. While seldom work is reported for the larger pitch cases, in which the grating diffraction still exits.

In this work, double layer aluminum gratings which have less fabrication process than the single layer cases are studied [10-11]. We show that the excitation and coupling of slit waveguide modes of the two layers leads to high transmission of TM light. The top metal layer helps to reflect back the TE light, thus improves extinction ratio, even when the slit width is larger than the cut-off width. In order to improve the transmission of TM light, an undercut structure is proposed [12]. The reason of the enhancement is that the undercut structure makes more light to be confined near the metallic side walls of the slit waveguides, thus the SP mode coupling efficiency between the bottom and top metallic grating is increased. The revealed mechanism is helpful in the new metallic nanowire polarizer design. Moreover, when the pitch is not too small, due to the SPRs on the substrate, sharp dips in the transmission spectra can be obtained [13]. The simultaneous SPRs can give a hint of designing an ultra compact thin film of reflective color filter and polarizer, which will be found applications in LCDs for power saving by taking place the conventional absorptive ones, which consume 60% and 50% of light passing through, respectively.

Passive Components and Fiber-Based Devices VIII, edited by Bishnu P. Pal, Proc. of SPIE-OSA-IEEE Asia Communications and Photonics, SPIE Vol. 8307, 830713
 · CCC code: 0277-786X/11/$18 · doi: 10.1117/12.904042

The structure of the double layer grating and the schematic of the SPRs are shown in Fig.1. The permittivities of air, dielectric slits, and substrate are ε_0=1, ε_1=2.25, and ε_s=2.25, respectively. The height of the dielectric is h. The top and bottom widths of the slits are t_1 and t_2. The pitch of the graing is T. Δh represents the step between two metal films. The metal chosen in this work is aluminum with permittivity ε_m described by Lorantz-Drude model with the plasmon frequency ω_p= 2.2758×10^{16} [14].

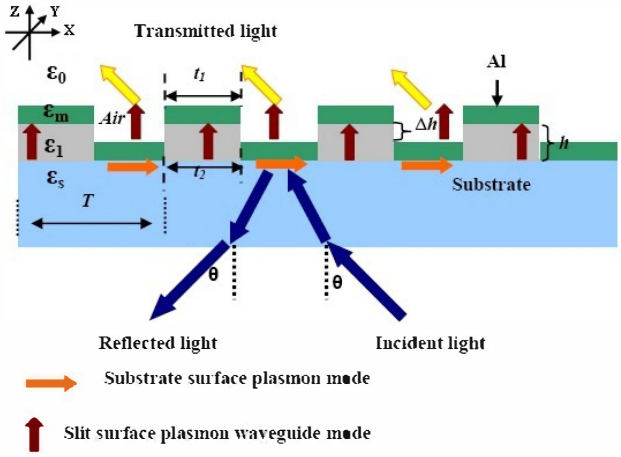

Fig.1 Sketch map of the double layer metallic nanowire grating and the surface plasmon mode resonance therein.

2. THEORY AND SIMULATION

2.1 Waveguide theory

As shown in Fig.1, because of the periodic character, the dispersion curves of the waveguide modes in the slits are described by photonic crystal dispersion as follows [15]:

$$\cos(KT) = \cos(k_1 l_1)\cos(k_2 l_2) - 1/2(g + 1/g)\sin(k_1 l_1)\sin(k_2 l_2) \quad (1)$$

where, K denotes the Bloch wave number, T is the pitch of the grating. l_1 =$\mathbf{t_1}$ and l_2 =T- $\mathbf{t_1}$ are the width of the dielectric and air slits, respectively, $k_1=(k_0^2\varepsilon_1-k_z^2)^{1/2}$ and $k_2=(k_0^2\varepsilon_m-k_z^2)^{1/2}$ are the wave number in the dielectric and aluminum along the X direction, respectively. k_z is the wave number of the waveguide mode along the Z axis. g =$k_1\varepsilon_m/(k_2\varepsilon_1)$ for TM light and k_1/k_2 for TE light.

The complex solutions of the two lowest order waveguide modes of metal-dielectric-metal on the bottom layer and the metal-air-metal at the top layer are shown in Fig. 2. The pitch T is 200nm and the slit width t_1 is 100nm. In solving equation (1), the maximum of the imaginary parts Kz_i is set to 0.4. The blue dot lines represent real parts of the solutions, while the red ones are imaginary parts. The black lines in the figures represent the dielectric and air lines of the slits. The real part solutions beneath the dielectric lines are SP waveguide modes, while, those above them are the regular waveguide modes. For the lines of imaginary solutions in each figure, the near zero line corresponds to the SP waveguide modes, while the other corresponds to the second order. For the second order, when the frequencies decrease, the imaginary parts become larger and larger, while the real parts get closer to zero. Once the imaginary parts are comparable to the real ones, it means that those solutions are dissipated and the waveguide modes are cut-off. As shown in Fig. 2(a), the cut-off frequencies of the second order is about 0.22ω_p, i.e. 376nm in wavelength. For the air slits of the top layer, the refractive index is smaller than that of the dielectric of the bottom layer, so the single mode cut-off frequency is larger than that of the bottom layer. As shown in Fig. 2(b), it is 0.33ω_p, corresponding to 250nm of wavelength. Because the dispersion curve of the first order of TE light is the same as that of the second order of TM light, it means that under the cut-off frequencies, only the SP modes are allowed to pass through. Thus, the grating can act as a polarizer in the whole visible light for LCDs.

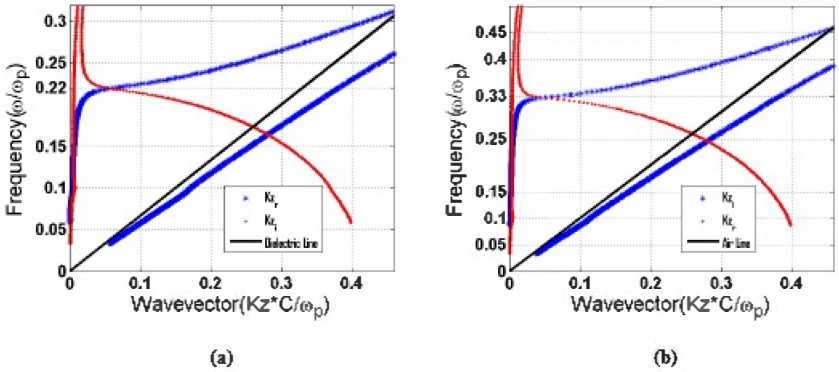

FIG.2. Dispersion curves of the waveguide modes of the **(a)** bottom and **(b)** top layers. The pitch T=200nm and l_1=l_2=100nm.

For the grating induced SP resonances on the metal surfaces, they can be written as [16]:

$$k_0 \sin(\theta)\hat{x} + nG\hat{x} = k_0\sqrt{\frac{\varepsilon_i \varepsilon_m}{\varepsilon_i + \varepsilon_m}}\hat{x} \tag{2}$$

In equation (2), the right side is the SP dispersion on the interface between aluminum/air or aluminum/substrate, where the subscript i=0, s represents the case of air and substrate, respectively; n=±1, ±2, ..., is the diffraction order of the grating. G =2π/T is the unit of reciprocal grating vector. In this study, only the case of incident plane parallel to the grating vector is considered, i.e. the wave vector components in y direction are zero. Fig.3 shows wavelengths of excited SP waveguide modes on the interfaces of aluminum/air and aluminum/substrate under different incident angles. Only the ±1 diffraction orders are plotted, which correspond to negative and positive incident angles, respectively. For the higher orders, the wavelengths are smaller than 400nm which are not the interests in this work. As shown in Fig.3, for the finer pitch and lower ambient refractive index, the resonant wavelengths are smaller. When the incident light is normal to the film, there is no lateral SP waveguide mode excited in visible light for the 200nm pitch case, while it is 485nm for the case of 320nm. With the increase of the incident angles, for the -1 order, the resonance wavelengths increase, and for the other, it is on the contrary. Because of the symmetry, only SP waveguide mode along positive x axis is considered. Thus, when the incident angles are minus, it means -1 order diffraction causes the excitation and vice versa.

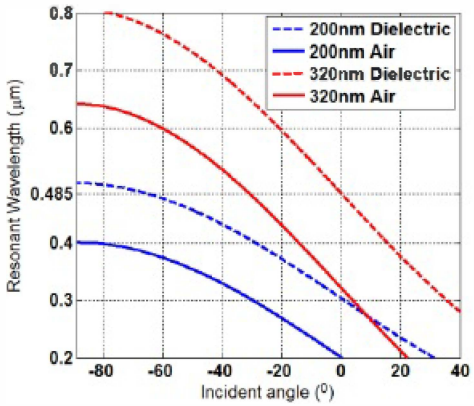

FIG. 3. Wavelengths of the excited surface plasmon waveguide modes on the interfaces of aluminum/air and aluminum/substrate under different incident angles.

From the above theoretical analysis, it is clear to see that there are two kinds of waveguide modes in the grating. Because of the SPR in the slits, the first order TM light is always sustained, while the first order TE light will be cut-off at a

minima wavelength for a specific slit width. For the SPRs on the lateral interfaces, they depend on the pitch and incident angles. Generally, with the decrease of the pitch, the resonant wavelengths will become shorter, which is suitable for wide band polarizers. When the pitch is not too small for the lateral SPRs to take away the light on resonance, the color filter and polarizer functions will be fulfilled in a single grating.

2.2 Simulation and Optimization

2.2.1 Polarizer

In order to obtain the spectra characters and optimize the performance of the as discussed devices, Finite-difference - time-domain (FDTD) method [17] is used for simulation. The transmittances of TM and TE light are shown in Fig.4 for pitch T = 200 nm, slit width t_1, t_2 = 100 nm, height h = 100 nm, and step Δh =10-40 nm. We can see that there is a distinct difference between the TM and TE light. The transmittance of TM light is larger than 30% in the whole visible spectrum. For the steps of 20 and 30nm, the TM transmission of shorter wavelengths can be improved to more than 60%. While in all the cases the maximum transmittance of TE light is just no more than 5%. The ratios of TM to TE transmission are several tens at least. Fig. 5 and 6 illustrate the corresponding field profiles and Z direction energy flux of TM and TE polarizations of Δh =30nm. For the TE polarization shown in Fig. 5, almost all the light is reflected back without entering the dielectric slits. This result agrees with the theoretical analysis in Fig.2 (a) that the TE modes are cut-off at this width. While for the TM polarization shown in Fig. 6, the incident light firstly couples to the bottom slit SP waveguide mode with highest field intensity nearby the dielectric-aluminum interface, then couples to the surface plasmon mode of the top layer with most of energy localized at the aluminum walls by near field scattering through the steps between the aluminum layers.

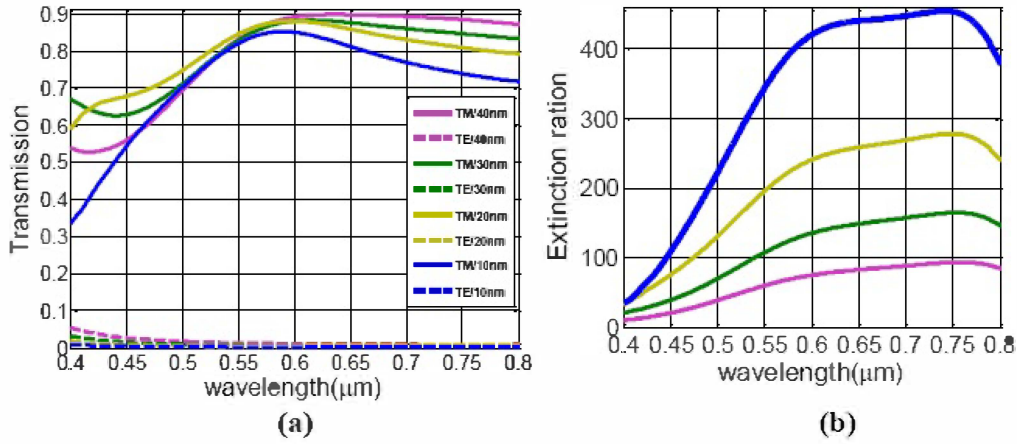

Fig. 4. Transmittance (a) and extinction ratio (b) of the TM/TE polarization with steps Δh from10 nm to 40 nm, both photoresist width w_1 and w_2 =100 nm, and height h =100 nm.

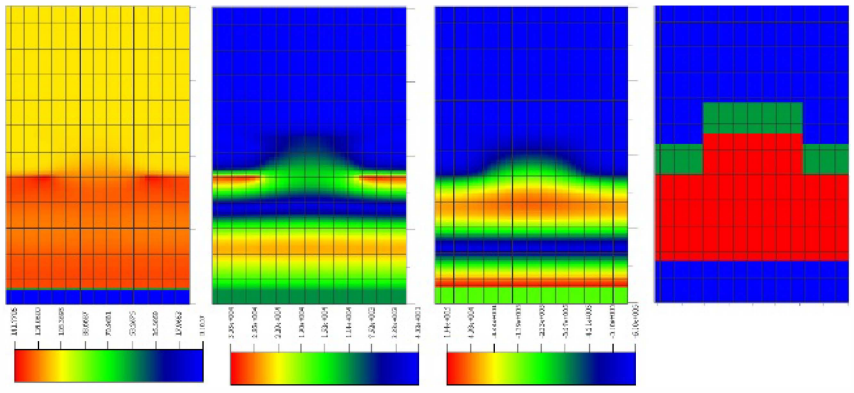

(a) Ex (b) Hy (c) Sz (d)

Fig. 5. Field profiles, energy flux and simulated structure of the plane wave TE polarized light incident from the bottom with Δh =30nm.

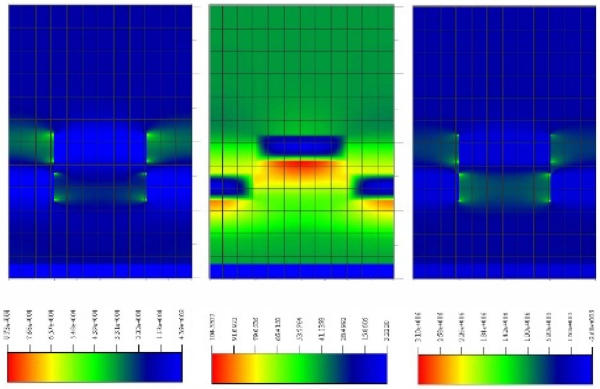

Fig. 6. Field profiles and energy flux of the plane wave TM polarized light incident from the bottom with Δh =30nm.

AS shown in Fig.6, for increasing the near field coupling efficiency, it is important to couple more incident light to the spacings between the metal layers. We find that the undercut structure of dielectric can facilitate this process. The structure can be obtained using lift-off photoresist which has an undercut profile with appropriate development. Fig. 7 shows the transmittance of the polarizer with width t_1 =100 nm, and t_2=40-80 nm. By comparison with Fig. 4 (a), one can see that the TM transmissions of the four cases increase in general. In order to explain the simulation results more clearly, the field profiles and energy flux of TM polarization with a metal step Δh of 20 nm are plotted in Fig.8. Compared with Fig. 6, it is clearly shown that, when the photoresist has an undercut profile, the incident light is reflected by the undercut structure of the photoresist and couples to the SP waveguide mode with more energy confined around the photoresist-aluminum interface. Thus, near field coupling through the spacing is increased and the transmittance of the TM polarization is improved.

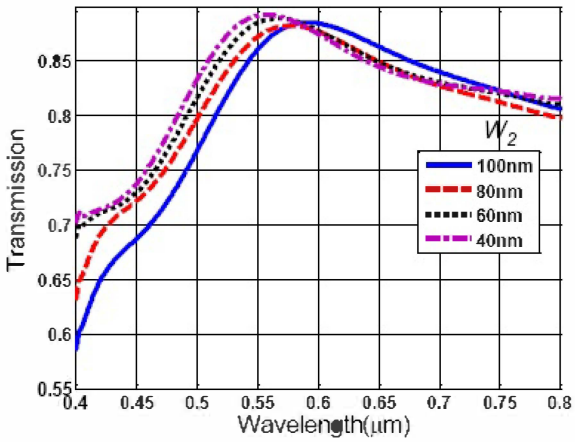

Fig. 7. Transmittance of the trapezoid photoresist nanowire polarizer with t_1 =100 nm, t_2 =40-100 nm, and step Δh =20 nm.

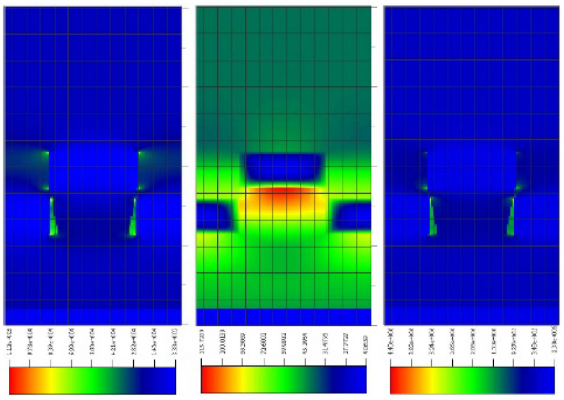

Fig. 8. Field profiles and energy flux of the plane wave TM light incident to the undercut profile photoresist polarizer with t_1=100 nm, t_2= 80 nm, and step Δh 20 nm.

2.2.2 Integrated color filters and polarizers

As depicted by the theory, if the pitch of the grating is not small enough, there will be diffraction caused lateral SPRs. Fig.3 gives an example of grating with pitch T of 320nm. The resonant wavelength at normal incidence is 485nm. The simulated transmission of the grating is shown in Fig. 9 with slit width t_1, t_2 = 130 nm, height h = 150 nm, and step Δh =10-80 nm. The slit width is chosen to be 130nm for the consideration of both single mode condition and light coupling efficiency for incident light. The detailed will be discussed in other work. We can see that, similar to as that of the 200nm pitch one, the polarization character is still maintained. The difference is that there is a dip in the transmission with center wavelength of about 495nm, which is close to the theoretical analysis. It means that because of the lateral SPR on the substrate, incident light does not pass through the film, but propagating along the substrate or reflected back. The cyan arrow in the figure illustrates the tendency of the spectra with increase of steps. The dip positions are not changed. The transmitted peak wavelengths of TM light are bluely shifted and the transmittances are raised at first and then declined at 80nm. The TE light transmissions are increased monotonously. For simultaneous high TM transmissions and TM/TE ratios, the step height Δh =30-60 nm is desirable. In a word, it is possible to make the color filter and polarizer together on a metallic nanowire grating with the simultaneous lateral and longitudinal SPRs.

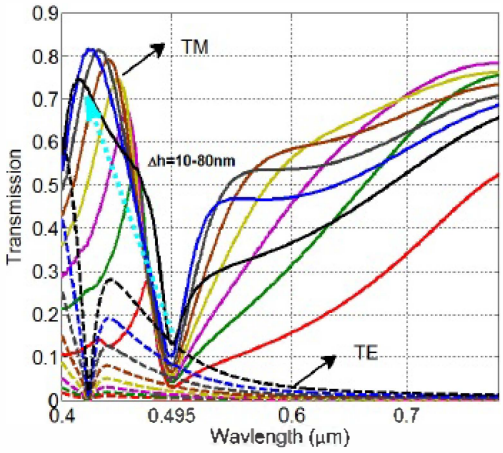

Fig. 9 The transmissions of the bi-layer grating with slit width t_1, t_2 = 130 nm, height h = 150 nm, and step Δh =10-80 nm

3. EXPERIMENT

For further checking of the simulations, bi-layer aluminum nanowire gratings are fabricated by laser interference lithography and E-beam deposition. The laser used is He-Cd laset (KIMMON) with the wavelength of 442nm. The E-beam depositor is Ei-5Z (ULVAC). The optical pictures of the fabricated sample are shown in Fig. 10. The sample size is $5\times 5cm^2$. The AFM (atomic force microscopy) and SEM (scanning electronic microscopy) images of the grating before and after Al deposition are shown in Fig. 11. We can see that the sample is not smooth enough and the line width of the grating is 200nm. It means that the exposure is not enough. The max height of the grating is about 150nm. In order to compromise, the height of the deposited Al is 70nm.

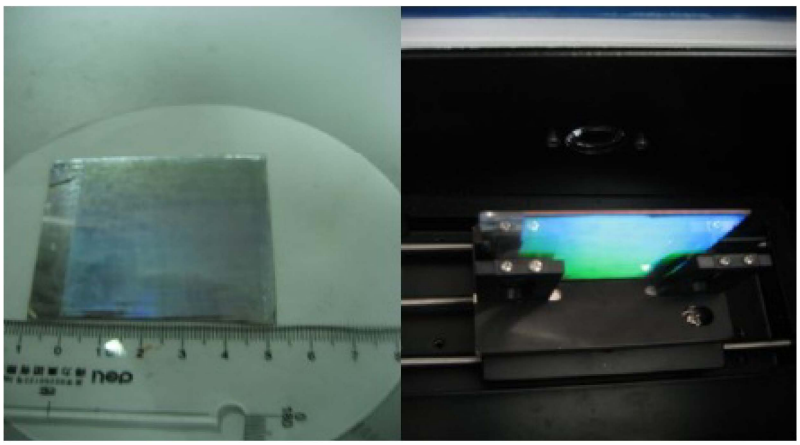

Fig. 10 Optical pictures of the fabricated grating with pitch of 320nm

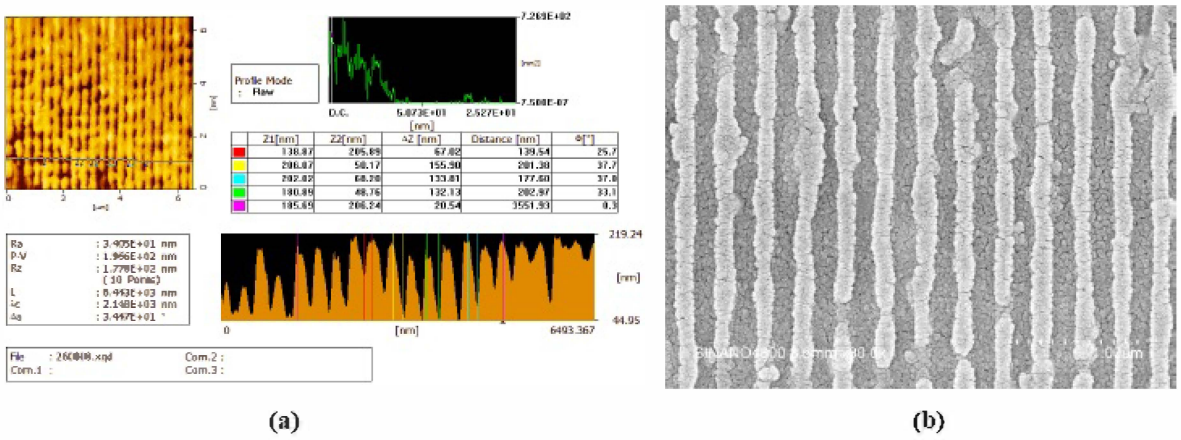

Fig. 11 The AFM (a) and SEM (b) image of the fabricated grating before and after Al deposition

The TM and TE spectra under different incident angles are measured using a HR4000 spectrometer (Ocean Optics) and shown in Fig. 12. We can see that the TM transmission is much higher than that of the TE. There are dips in the TM spectra, which are shifted to longer wavelengths with the increase of incident angles. By comparison with Fig. 3 of -1 order case, the measurements are coincident with the theoretical calculations. Actually, there should be dips corresponding to +1 order, which will be shifted to shorter wavelengths . However, because of the low efficiency of the light source in the blue light, it can not be clearly shown in this measurement. Further measurement will be taken in the future.

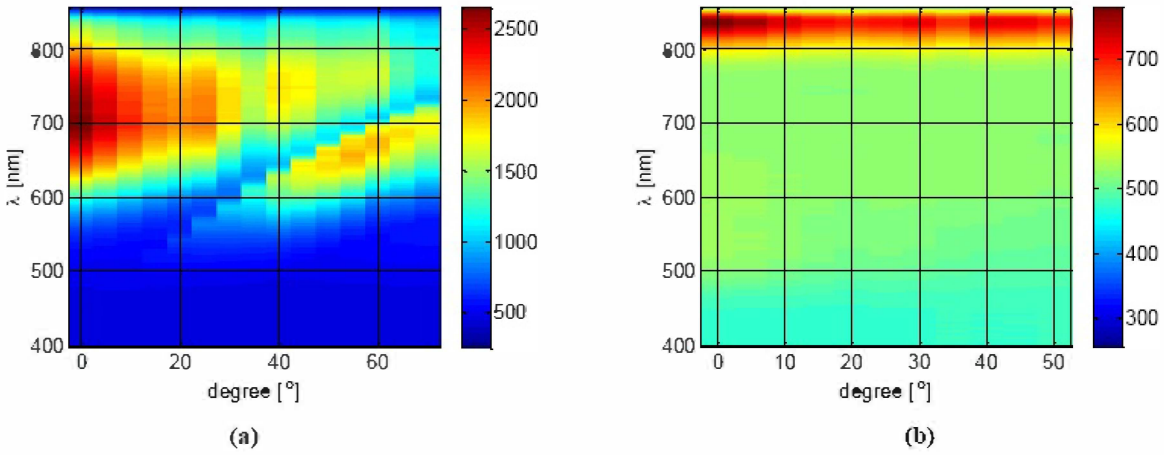

Fig. 12 Transmissions of the TM (a) and TE (b) light under different incident angles

4. CONCLUSION

The mechanism of the two kinds of surface plasmon resonances in the metallic nanowire gratings is analyzed both in theoretical calculation and numerical simulation. The longitude slit SP waveguide resonance is responsible for the high TM polarized transmittance and the lateral resonance leads to the dips in the transmitted spectra. With the coinstantaneous resonances, a double-function grating is proposed and optimized. The fabrication and measurement of the devices verify the design further. In conclusion, we have proved both in theory and experiment that by utilizing lateral and longitude SPRs, it is possible to fabricate ultra compacted reflective color filters and polarizers of a single bi-layer metallic nanowire grating. This work will be very important for applications in LCDs for power saving by taking place of the conventional absorptive ones.

5. ACKNOWLEDGEMENT

This work was supported by the National Natural Science Foundation of China (Grant No. 61007025, 60906039, 11004037), Shanghai Natural Science Foundation (Grant No.09ZR1414800), and Ministry of Education (20100073120034). The authors acknowledge Infovision Optoelectronics Company (IVO) for financial support. The aluminum deposition was carried out in Suzhou Institute of Nano-tech and Nano-bionics. The AFM was measured in Instrumental Analysis Center of Shanghai Jiao Tong University.

REFERENCES

[1] Pei-Yu Chung, Tzung-Hua Lin, Gregory Schultz, Christopher Batich, and Peng Jiang, Appl. Phys. Lett. **96**, 261108 (2010).
[2] D. M. Koller, A. Hohenau, H. Ditlbacher, N. Galler, F. Reil, F. R. Aussenegg, A. Leitner, E. J. W. List, and J. R. Krenn, Nature Photon. **2**, 684 (2008).
[3] K.R. Catchpole, and A. Polman, Opt. Express. **16**, 21793 (2008).
[4] R. F. Oulton, V. J. Sorger, D. A. Genov, D. F. P. Pile, and X. Zhang, Nature Photon. **2**, 496 (2008).
[5] C. Tsai and S. Wu, Appl. Opt. **47**, 2882–2887 (2008).
[6] Eric Laux, Cyriaque Genet, Torbjorn Skauli, and Thomas W. Ebbesen, Nature Photon. **2**,161 (2008)
[7] I. I. Smolyaninov, Y.-J. Hung, and C. C. Davis, Appl. Phys. Lett. **87**, 241106 (2005).
[8] Sang Hoon Kim, Joo-Do Park, and Ki-Dong Lee, Nanotechnology **17**, 4436-4438 (2006).
[9] Hiroshi Kawamoto, "The history of liquid-crystal displays," Proceedings of the IEEE **90**, 460–500 (2002).
[10] A. G. Lopez, and H. G. Craighead, Opt. Lett. **23**, 1627-1629 (1998).
[11] Se Hyun Ahn, and L. Jay Guo, **20**, 2044-2049 (2008).
[12] Zhicheng Ye, Yao Peng, Tianrui Zhai, Ying Zhou, and Dahe Liu, J. Opt. Soc. Am. B. **28**, 502 (2011)
[13] Zhicheng Ye, Jun Zheng, et al, Submitted

[14] E. D. Palik, Handbook of Optical Constants of Solids (Academic, 1985).
[15] Zhicheng Ye, Jun Zheng, Zhaona Wang, and Dahe Liu, Solid State Commun. **136**, 495 (2005).
[16] Igor I. Smolyaninov,a_ Yu-Ju Hung, and Christopher C. Davis, Appl. Phys. Lett. **87**, 241106 (2005)
[17] A. Taflove, and S. C. Hagness, *Computational Electrodynamics: The finite-difference time-domain method* (Artech House, 2005).